Journal of the Korean Society for Nondestructive Testing
Vol. 27, No. 6 (2007. 12)

Parametric and Wavelet Analyses of Acoustic Emission Signals for the Identification of Failure Modes in CFRP Composites Using PZT and PVDF Sensors

Kritsada Prasopchaichana* and Oh-Yang Kwon*,†

Abstract Combination of the parametric and the wavelet analyses of acoustic emission (AE) signals was applied to identify the failure modes in carbon fiber reinforced plastic (CFRP) composite laminates during tensile testing. AE signals detected by surface mounted lead-zirconate-titanate (PZT) and polyvinylidene fluoride (PVDF) sensors were analyzed by parametric analysis based on the time of occurrence which classifies AE signals corresponding to failure modes. The frequency band level-energy analysis can distinguish the dominant frequency band for each failure mode. It was observed that the same type of failure mechanism produced signals with different characteristics depending on the stacking sequences and the type of sensors. This indicates that the proposed method can identify the failure modes of the signals if the stacking sequences and the sensors used are known.

Keywords: Acoustic Emission, Wavelet, Composites, Failure Modes

1. Introduction

The failure modes in composite materials are more complex than in metals because composite materials experience several damage mechanisms under stress, such as fiber breakage, interface debonding, and matrix cracking, that can cause degradation in mechanical properties. Among non-destructive evaluation (NDE) methods for failure modes identification in composites, the acoustic emission (AE) technique has been extensively used for real-time damage monitoring. AE is an elastic wave generated by the rapid release of strain energy from various sources within a material. This elastic wave can be detected and monitored by sensors to provide the valuable information about the AE source location and characteristics which are associated with the structural failure analysis. AE signals in composite materials result mainly from the energy release of failure modes. So, parameters and waveforms of AE signals become important in monitoring and detecting failure modes.

Conventional AE sensors are made of piezoelectric ceramics, especially lead-zirconate-titanate (PZT), which has high sensitivity and can be applied to a wide range of the structure materials. Although a second sensor, the polyvinylidene fluoride (PVDF) film sensor, exhibits lower sensitivity as compared to PZT, it is still recognized as a potential sensor that overcomes the limitations of PZT specifically, its brittle nature and thickness. PVDF film can be effectively used as an AE sensor and directly attached or embedded to the structure materials without disturbing its mechanical motion(Kwon and Dzenis, 2004; Park et al., 2005; Bar et al., 2004, 2005)

Received: October 5, 2007, Accepted: November 26, 2007. * Department of Mechanical Engineering, Inha University, Incheon 402-751, South Korea, † Corresponding author: okwon@inha.ac.kr

The conventional method of AE parametric analysis based on the time of occurrence can identify the failure mechanism group in composite laminates (Bar et al., 2004, 2005; Johnson and Gudmundson, 2001; Johnson, 2002). However, for the various mechanisms, the AE signals overlap in their parameters distributions, which reduce the accuracy of results. Thus, many authors have improved the identification of damage modes by processing AE signal parameters in several methods, such as principal component analysis (Johnson, 2002), artificial neural network(Bar et al., 2004; Huguet, 2002) and wavelet analysis (Qi, 2000; Ni and Iwamoto, 2002; Loutas et al., 2006). Wavelet analysis is applied in AE signal processing for several purposes, such as analysis of plate wave propagation in anisotropic laminates (Jeong, 2001), waveform analysis for estimating AE wave arrival times (Ding et al., 2004), and failure modes identification. In data reported in the literature, wavelet analysis using the wavelet transform extracts AE signals to time-frequency information that can be used to determine which failure mode occur prior to the others (Ni and Iwamoto, 2002). The wavelet-based AE analysis using discrete wavelet supports the widely accepted aspect that each failure mechanism is characterized by a certain frequency band level-energy analysis (Qi, 2000; Loutas et al., 2006).

The widely accepted aspect regarding parametric analysis of AE signals show that each failure mechanism can be characterized by simple waveform parameters which provide an indication of source intensity or severity. In many cases, AE testing also detects unwanted background noise that cannot be removed by conventional signal conditioning. Therefore, it is necessary to identify the source of each signal as it received. In this paper, AE signals detected by both PZT and PVDF film sensors were filtered by bandwidth, threshold level and geometrical filter techniques. Then, filtered signals were analyzed by the combination of the parametric and the wavelet analyses in terms of a certain frequency band-energy to identify the failure modes in carbon fiber reinforced plastic (CFRP) composite.

2. Experimental Procedure

The specimens were produced from a unidirectional carbon/epoxy prepreg (UHN125C, Sky Flex). The tensile strength and modulus of the carbon fiber are 4.61 GPa and 392.4 GPa respectively and the epoxy resin content of the prepreg is 30 %. Three laminates of different lay-up sequences $[0^\circ]_8$ (unidirectional laminates), $[0^\circ/90^\circ]_{2S}$ (cross-ply laminates) and $[\pm45^\circ]_{2S}$ (angle-ply laminates) were prepared in a vacuum-bagged setting and cured in an autoclave at 82 °C for 30 minutes and then at 121 °C for 90 minutes under a pressure of 500 kPa. The tested specimens had a length of 250 mm, a width of 25 mm, a thickness of 0.9 mm and double-end notches of width 8 mm at the middle length of specimen. They were all wet sanded in order to prevent damage initiations from edge effects introduced by the cutting process. The tabs were 40 mm in length, 25 mm in width and had a thickness of about 3 mm. For the $[0^\circ]_8$ specimens, they were increased layer $[\pm45^\circ]_2$ on each side as shown in Fig. 1. This was done in order to prevent splitting along specimens that break the contact between the sensor and specimen surface.

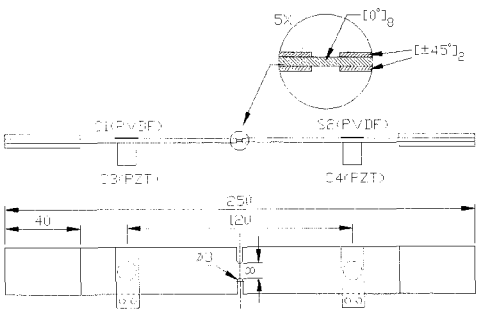

Fig. 1 Test specimen of unidirectional laminates with sensor positions

The specimens were tensile tested on a table-top testing machine (TIRAtest 27025, TIRA Maschinenbau GmbH). The crosshead speed was set to 0.2 mm/min. Two PVDF film sensors of thickness 28 μm and two PZT sensors (B1025, Digital Wave Corp.) were mounted equi-distant 60 mm from the double-end notches as shown in Fig. 1. The acoustic emissions were continuously monitored during tensile testing using an AE data acquisition system (Mistras 2001, Physical Acoustics Corp.), with a sampling rate of 4 MHz, pre-amplification of +40 dB, band-pass filtering of 0.1-1.2 MHz and threshold of 55 dB.

Wave velocity in the CFRP was measured by both of two attached PVDF sensors and two PZT sensors with 30 mm distance apart in one dimensional plate specimen as shown in Fig. 2(a). AE sources were generated by the pencil-lead-break method. The difference in the arrival time, Δt, was measured by using built-in AE software. The wave velocity was calculated by the measurement of Δt, which is given as

$$\Delta t = \frac{D}{V} \tag{1}$$

where D is the distance between sensors and V is the constant wave velocity.

Linear location of an acoustic emission source between sensors, the source location d in Fig. 2(b) is given as (Miller and McIntire, 1987)

$$d = \frac{1}{2}(D - \Delta t V) \tag{2}$$

where d is measured from the first hit sensor. The difference in arrival time between the sensors in the case of source location at the boundary of the double-end-notched area = $\frac{(D+x)}{2V} - \frac{(D-x)}{2V} = \frac{x}{V}$

In the data acquisition system, an AE channel detected and processed an AE transient in terms of an AE hit. There were many AE hits detected by 4 channels during tensile testing which included AE from areas of interest and of no interest, noise from grips, etc., therefore an event lockout time was necessary to resume event processing within a group. This time should be at least as long as the time it takes for an AE event to propagate from one sensor to the last or furthest sensor in a given group. In this study, the area of interest was the double-end-notched area of 8×3 mm, the maximum different distance from the source within an area of interest to two sensors located opposite each other was 3 mm. So event lockout time was the time that a wave propagates through 3 mm. The wave velocity for each lay-up sequence specimen had to be determined before the tensile test to calculate event lockout time. After obtaining data, the noise and signals from areas of no interest were eliminated by the event lockout time programming (using a geometrical filter technique). The exact events within the area of interest were only considered.

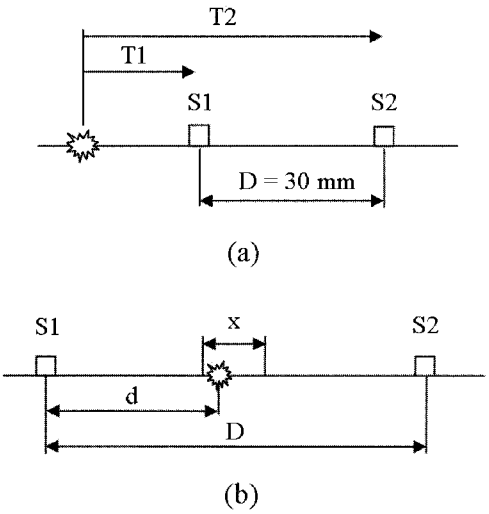

Fig. 2 (a) wave velocity measurement; (b) linear source location technique

3. Frequency Band-Energy Analysis Based on Wavelet Packet Transform

Wavelet transform is a powerful tool for the Time-Scale-Analysis that has been introduced

over the last 15 years in order to overcome the limited time-frequency localization of the Fourier-transformation (FT) for non-stationary signals. Wavelet analysis has found a lot of applications in signal and image processing which include the suitability of AE signal analysis.

In wavelet analysis, the signal is decomposed to approximations and details. The approximations are the high-scale, low-frequency components of the signal and the details are the low-scale, high-frequency components. The decomposition process can be iterated, with successive approximations being decomposed in turn, so that one signal is broken down into many lower resolution components. This is called the wavelet decomposition tree as shown in Fig. 3 (Qi, 2000; Misiti et al., 2000).

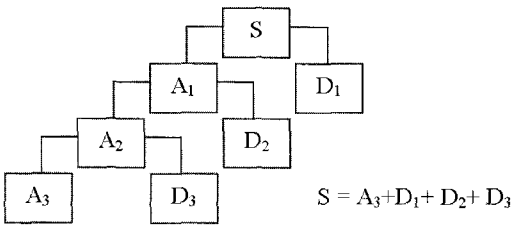

Fig. 3 The 3-level wavelet decomposition tree

In wavelet packet analysis, the details as well as the approximations can be split. Therefore, the wavelet packet method is a generalization of wavelet decomposition that offers a richer range of possibilities for signal analysis. The complete binary tree is produced as shown in the following Fig. 4 (Misiti et al., 2000). The idea of this decomposition is to start from a scale-oriented decomposition, and then to analyze the obtained signals on frequency subbands. In this study, the name of wavelet packet are named by numbers of level and order enclosed in parentheses, for example, the wavelet packet AAA3, DAA3, ···, and DDD3 are named wavelet packet (3,0), (3,1),···, and (3,7) respectively.

MATLAB was used to apply the wavelet packet transform to AE waveforms because it provides a versatile wavelet toolbox and also offers the possibility of programming. After all AE waveforms were loaded into MATLAB, wavelet pack transform was applied to every signal to decompose the original AE signal into its wavelet packets. Decomposition was based on 'db20' wavelet (member of the Daubechies wavelets family) and five levels of analysis. Therefore, each signal was decomposed to 32 wavelet packets, namely wavelet packet (5,0), (5,1),···, (5, 31) which are represented at frequency band [0-62.5], [62.5-125], ···, [1937.5-2000] kHz, respectively. Because the AE signals were acquired at sampling rate of 4 MHz, so frequencies up to 2 MHz were considered. Obviously, the wavelet packet (5,1), (5,2), ···, (5,19) correspond frequency band of 62.6-1250 kHz which cover the band pass filter 100-1200 kHz. This means wavelet packet (5,1), (5,2), ···, (5,19) are sufficient for analysis in this work. The family of Daubechies wavelets was chosen because it consists of biorthogonal, compactly supported wavelets, satisfactorily regular though not symmetrical, which are

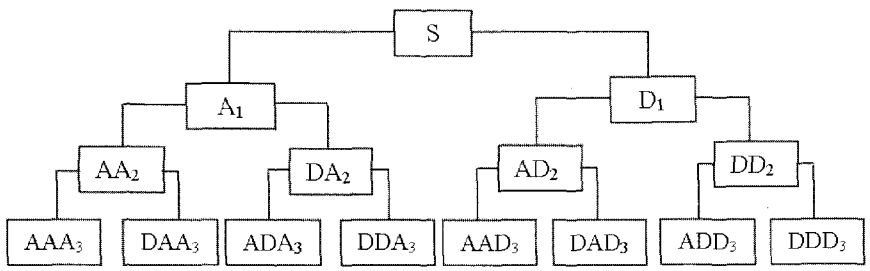

Fig. 4 Wavelet packet decomposition tree at level 3

important for the analysis of transient AE signal activity (Loutas et al., 2006).

The energy content of the acoustic emission signal can be related to the electrical energy U which is presented in a transient event (Miller and McIntire, 1987)

$$U = \frac{1}{R}\int_0^\infty V^2(t)dt \tag{3}$$

where R is the electrical resistance of the measuring circuit. Regardless of the definition of energy measurement used, none is an absolute energy quantity. They are relative quantities proportional to the true energy. So, the constant R can be neglected for comparison. In this study, after the decomposition of all AE signals, the energy content of each wavelet packet is calculated by sum of the square of the time series $f^{(i)}(t)$, which is given as

$$E^{(i)}(t) = \sum_{t=t_0}^{t=t_n} (f^{(i)}(t))^2 \tag{4}$$

where $E^{(i)}(t)$ is the energy of wavelet packet i and $f^{(i)}(t)$ represents time series of wavelet packet i. The value of the energy content of each wavelet packet is difficult to compare. So, in this study, they were calculated in terms of percentage of the wavelet packet-energy as compared with the total energy of the AE signal.

4. Results and Discussion

4.1 Unidirectional Laminates

The typical amplitude distributions with increment of stress were plotted against time. The distribution of AE signal amplitude detected from the unidirectional laminates by the PVDF sensors is shown in Fig. 5. As can be observed, the first set of signals with amplitude below 65 dB is noticeable throughout the test. AE signals with amplitudes in the range of 65-75 dB are generated at between 70 and 100 % of the failure stress. The third set of signals with amplitude above 75 dB appears only near the failure stress.

The distribution of AE signal amplitude detected from the unidirectional laminates by the PZT sensors is shown in Fig. 6. The pattern of distribution is similar to that produced by the PVDF sensors but the PZT sensors detected more signals than the PVDF sensors and also detected an average amplitude value that was higher than the value given by the PVDF sensors due to higher sensitivity. It can be observed that the set of signals, which has amplitude below 75 dB, appears over the entire stress period. At higher stress levels, AE signals with amplitude range of 75-85 dB are generated between 70 and 100 % of the failure stress. The last set of signals with amplitude above 85 dB is presented only near the failure stress.

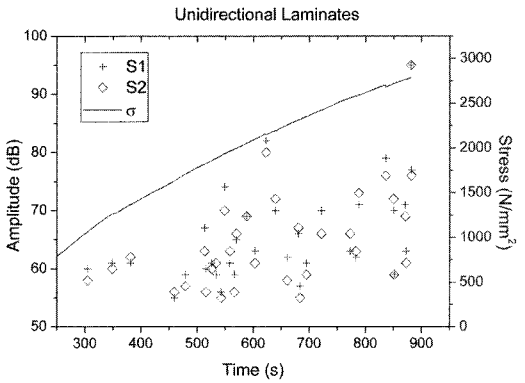

Fig. 5 AE signal amplitude distribution detected from unidirectional laminates by PVDF sensors

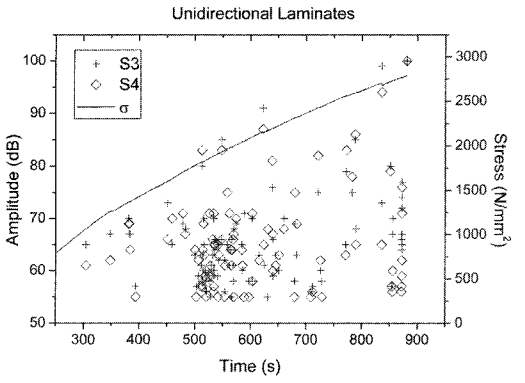

Fig. 6 AE signal amplitude distribution detected from unidirectional laminates by PZT sensors

On the basis of the time of occurrence (Bar et al., 2004, 2005; Johnson and Gudmundson, 2001; Johnson, 2002), the distribution of AE signal amplitude detected from the unidirectional laminates by the PVDF sensors can be observed that the first set of signals with amplitude below 65 dB characterize matrix cracking, while the second set of 65-75 dB corresponds to interface debonding, and the remaining higher values are produced by fiber fracture. A certain frequency band-energy analysis was applied on all signals and the average percentages of wavelet packet-energy are calculated according to signal amplitude ranges which respond to the failure mechanism based on the aforementioned as shown in Fig. 7. In this study, the dominant frequency bands are the top few wavelet packet-energies which are summed up at least 50 % of the total energy. For example, from Fig. 7 (a), it can be observed that the set of signals with amplitude below 65 dB have the top three wavelet packet-energies at wavelet packet (5,1), (5,2) and (5,3) which are aggregated about 52.79 % of the total energy. This means the dominant frequency band for matrix cracking is at 62.5-250 kHz. Fig. 7 (b) shows the set of amplitudes in the 65-75 dB range has the top three wavelet packet-energies at wavelet packet

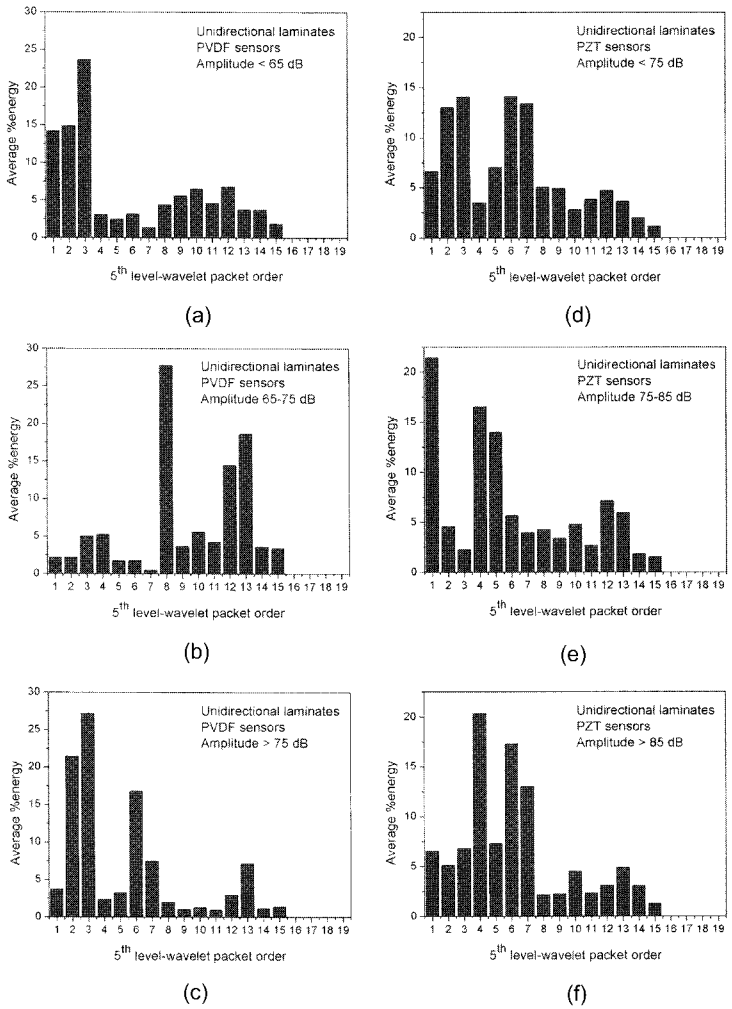

Fig. 7 The results of the parametric and wavelet analyzes of AE signals detected from unidirectional laminates by PVDF and PZT sensors

(5,8), (5,12) and (5,13) about 60.83 % of the total energy. So, the main frequency bands for interface debonding are 500-562.5 and 750-875 kHz. Fig. 7 (c) shows that the set of signals with amplitude above 75 dB has the dominant frequency bands at 125-250 and 375-437.5 kHz, about 65.45 % of the total energy, which correspond to fiber fracture.

The results of the parametric and wavelet analyzes of AE signals detected from unidirectional laminates by PZT sensors are shown in Fig. 7 (d)-(f). The first set of amplitudes below 75 dB shows the main frequency band at 125-250 and 375-500 kHz. The second set of amplitudes in the range of 75-85 dB has its dominant frequency bands at 62.5-125 and 250-375 kHz. The last set of amplitudes above 85 dB present the dominant frequency band at 250-312.5 and 375-500 kHz. On the basis of the time of occurrence, the three sets of AE signals correspond to the failure mechanisms matrix cracking, interface debonding and fiber fracture, respectively.

The results of both PVDF and PZT sensors clearly indicate that for the signals in same damage mode, the dominant frequency band for the PZT sensor is different to the PVDF sensor, due to the different material properties of the sensors used.

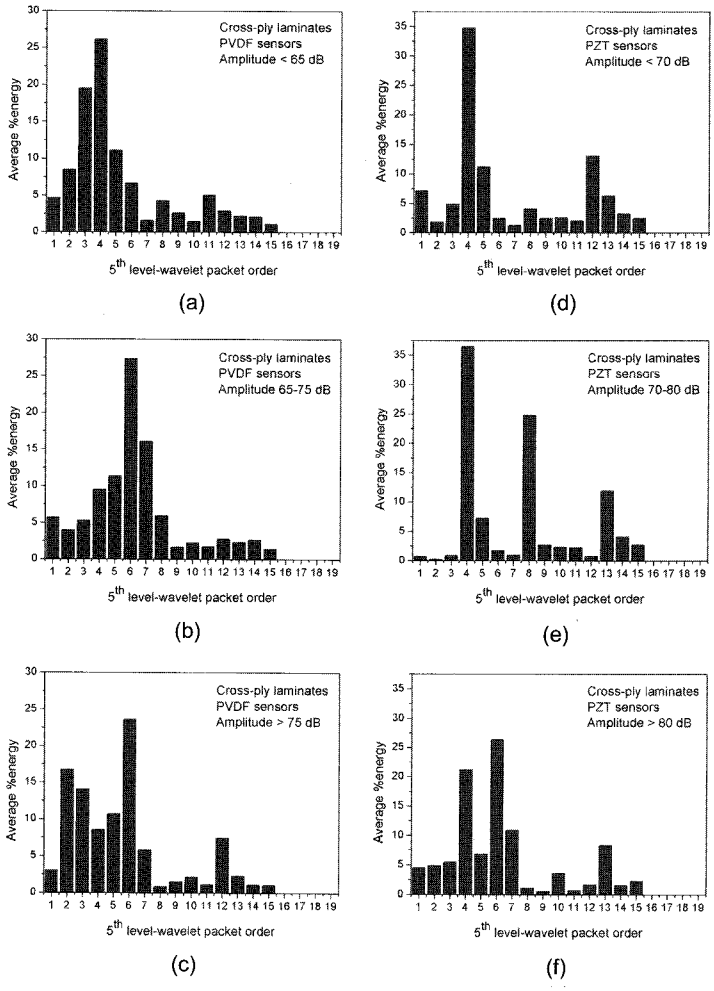

Fig. 8 The results of the parametric and wavelet analyzes of AE signals detected from cross-ply laminates by PVDF and PZT sensors

4.2 Cross-Ply Laminates

The AE signals detected from the cross-ply laminates by PVDF sensors were analyzed in terms of the average percentages of wavelet packet-energy according to amplitude ranges which are classified by the parametric analysis of amplitude distribution. The results are shown in Fig. 8 (a)-(c), it is evident that the set of amplitudes below 65 dB shows the main frequency band at 187.5-375 kHz, for the set of amplitudes in the range 65-75 dB, the dominant frequency band is at 312.5-500 kHz, and the set of amplitudes above 75 dB present the dominant frequency bands at 125-250 and 375-437.5 kHz.

Fig. 8 (d)-(f) shows the results of the parametric and wavelet analyses of AE signals detected from cross-ply laminates by PZT sensors. As can be observed, the first set of amplitudes below 70 dB has its dominant frequency band at 250-375 and 750-812.5 kHz. The second set of amplitudes, which is in the range of 70-80 dB, has a major frequency band at 312.5-500 kHz and the last set of amplitudes above 80 dB presents the dominant frequency band at 250-312.5 and 375-500 kHz. In the literature (Bar et al., 2004, 2005; Johnson and Gudmundson, 2001; Johnson, 2002), there are

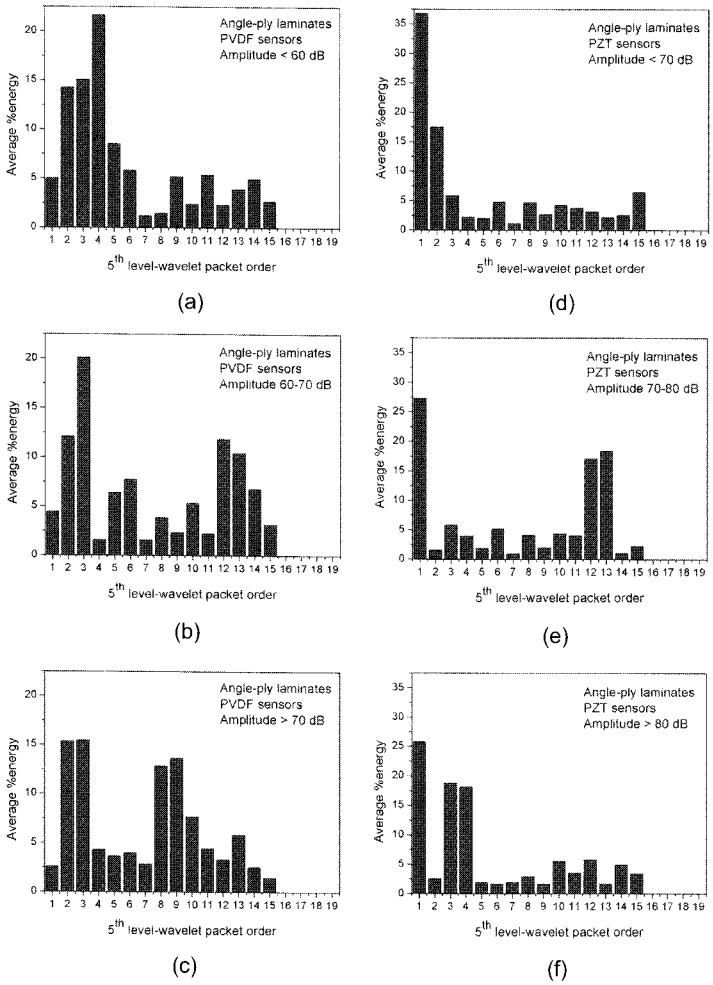

Fig. 9 The results of the parametric and wavelet analyzes of AE signals detected from angle-ply laminates by PVDF and PZT sensors

three dominant failure mechanisms occurring in cross-ply composites under tensile load. These are transverse matrix cracking, interface debonding and fiber fracture. On the basis of time of occurrence, it can be inferred that the above mentioned failure mechanisms correspond to the set of low, medium and high amplitude of AE signals, respectively.

Comparing the results of cross-ply laminates with those for unidirectional laminates, there is a set of signals with maximum amplitude that has the same dominant frequency band in results of both PZT and PVDF sensors. It can be observed that in both unidirectional and cross-ply laminates, the 0^{o} plies mainly affect the occurrence of fiber fracture signals. Therefore, it can be concluded that for the same type of failure mechanism, the produced signals have different characteristics depending on the stacking sequences fabricated. Furthermore, the results of the cross-ply laminates test show that the dominant frequency band for the PZT sensor was different to the PVDF sensor, just as in unidirectional laminates test, even though the signals were produced from the same specimen and damage mode. This indicates that the different material properties of the sensors affect the frequency response.

4.3 Angle-Ply Laminates

The data obtained from the angle-ply laminate experiments were analyzed by the combination of the parametric and the wavelet analyses. Fig. 9 (a)-(c) shows the results for the AE signals detected from the angle-ply laminates by the PVDF sensors. As can be observed, the set of amplitudes below 60 dB has the major frequency band at 125-321.5 kHz. The set of amplitudes in the range of 60-70 dB has its dominant frequency bands at 125-250 and 750-875 kHz. The set of amplitude above 70 dB present the top four wavelet packet-energies at a frequency band of 125-250 and 500-625 kHz.

Based on the literature (Bar et al., 2004, 2005; Johnson and Gudmundson, 2001; Johnson, 2002), the results indicate that AE transients are generated because of matrix cracking at lower strain values and followed by the formation of a local delamination at the notch-root edge of the specimen when the load increase. At mostly end of the test, one of them starts to grow over the entire width of the specimen, resulting in final failure. These types of signals are not observed with other stacking sequences. Considering the time of occurrence, it can be assumed that the set of amplitude in the range of below 60 dB, 60-70 dB and above 70 dB, correspond to the failure mechanisms due to matrix cracking, local delamination and delamination progress, respectively.

The results of the parametric and wavelet analyses of AE signals detected from angle-ply laminates by the PZT sensors are shown in Fig. 9 (d)-(f). It can be seen that the set of amplitudes below 70 dB has its major frequency band at 62.5-187.5 kHz which corresponds to matrix cracking. The local delamination signals have the same dominant frequency band as matrix cracking at 62.5-125 kHz but also respond to the frequency band at 750-875 kHz. The set of amplitudes above 80 dB present the top three of wavelet packet-energies about 62.54 % at the frequency band 62.5-125 and 187.5-321.5 kHz as corresponds to the delamination progress.

Angle-ply composites generate larger numbers of AE events in a short period which are mostly overlapping and can be observed in both PZT and PVDF sensors. All of the failure mechanisms have overlapping dominant frequency bands at wavelet packet (5,2) and (5,3) in the results generated by the PVDF sensors and wavelet packet (5,1) for PZT sensors, but they can be characterized by the other wavelet packets of dominant frequency bands. Comparing the matrix cracking results of angle-ply laminates to unidirectional and

cross-ply laminates, the dominant frequency bands are significantly different. So, this indicates that the same type of failure mechanism produces signals with different characteristics depending on the stacking sequences.

4.4 Failure Modes Identified by Signal Analysis

The AE signals generated from different types of failure modes, such as fiber fracture, matrix cracking, interface debonding, local delamination and delamination progress in CFRP composites were presented. For the classification of the AE signals, combination of the parametric and the wavelet analyses was used. Among the three different stacking sequences of laminates, there is a set of signals with maximum amplitude in unidirectional and cross-ply laminates having the same dominant frequency band at wavelet packet (5,2), (5,3) and (5,6) for PVDF sensors and wavelet packet (5,4), (5,6) and (5,7) for PZT sensors. This is because both longitudinal and cross-ply laminates have the 0° plies which mainly contribute to the occurrence of fiber fracture signals.

Comparing the matrix cracking results among unidirectional, cross-ply and angle-ply laminates, it was seen that the same type of matrix cracking produced in unidirectional ply, cross-ply and angle-ply have significantly different dominant frequency bands depending on the crack orientations in terms of the location of the sensors. This can be explained by the fact that cracks in unidirectional laminates grow toward the sensors, cracks in cross-ply laminates grow transversely across the double-end notches area and cracks in angle-ply laminates grow toward from the transducers due to the fiber orientation. Another reason could be the differences in wave propagation characteristics according to lay-up sequence.

In addition, the interface debonding results in unidirectional and cross-ply laminates indicates that the dominant frequency bands are significantly different. This clearly indicates that same type of failure mechanism produces signals with different characteristics depending on the stacking sequences. For signals from the same specimen and damage mode, the dominant frequency band gotten for PZT sensors was different to PVDF sensors. This may indicate that different sensor material's properties affect frequency response differently.

Furthermore, for the delamination signals, a distinction between local delamination and delamination progress of the angle-ply lamination was observed from the average energy percentages of frequency band-wavelet packets. It was also seen that local delamination and delamination progress signals have overlapping dominant frequency bands at wavelet packet (5,2) and (5,3) for the PVDF sensors and wavelet packet (5,1) for the PZT sensors. But these can be discriminated using the fact that local delamination signals have another dominant frequency band at wavlet packet (5,12) and (5,13) for both the PVDF and PZT sensors. Delamination progress signals have another dominant frequency band at wavelet packet (5,8) and (5,9) for the PVDF sensors and wavelet packet (5,3) and (5,4) for the PZT sensors.

5. Conclusions

From the parametric analysis based on time of occurrence of peak amplitude distribution, sets of AE signals related to failure modes were classified. The average percentages of frequency band-energy which were extracted by the wavelet packet transform can distinguish the dominant frequency band for each failure mode. These investigations have shown that the same type of failure mechanism produces signals with different characteristics depending on the stacking sequences and the type of sensors used. By using the combination of the parametric and the wavelet analyses, if the stacking sequence under tensile load is known, the signals detected by PVDF or PZT sensors can be used to identify the failure modes. Failure modes identification

must be based on dominant frequency bands from the completely recorded results which cover the types of stacking sequence, load, sensor, and shape of the composite.

Acknowledgement

This work was supported by Inha University Research Grant (INHA-30296).

References

Bar, H. N., Bhat, M. R. and Murthy, C.R.L. (2004) Identification of Failure Modes in GFRP Using PVDF Sensors:ANN Approach, Composite Structures Vol. 65, pp. 231-237

Bar, H. N., Bhat, M. R. and Murthy, C.R.L. (2005) Parametric Analysis of Acoustic Emission Signals for Evaluating Damage in Composites Using a PVDF Film Sensor, Journal of Nondestructive Evaluation Vol. 24, No. 4, pp. 121-134

Ding, Y., Reuben, R. L. and Steel, J. A. (2004) A New Method for Waveform Analysis for Estimating AE Wave Arrival Times Using Wavelet Decomposition, NDT&E International Vol. 37, pp. 279-290

Huguet, S., Godin, N., Gaertner, R., Salmon, L. and Villard, D. (2002) Use of Acoustic Emission to Identify Damage Modes in Glass Fibre Reinforced Polyester, Composites Science and Technology Vol. 62, pp. 1433-1444

Jeong, H. (2001) Analysis of Plate Wave Propagation in Anisotropic Laminates Using a Wavelet Transform, NDT&E International Vol. 34, pp. 185-190

Johnson, M. and Gudmundson, P. (2001) Experimental and Theoretical Characterization of Acoustic Emission Transients in Composite Laminates, Composite Science and Technology Vol. 61, pp. 1367-1378

Johnson, M. (2002) Waveform Based Clustering and Classification of AE Transients in Composite Laminates Using Principal Component Analysis, NDT&E International Vol. 35, pp. 367-376

Kwon, O. and Dzenis Y.A. (2004) Embedded PVDF Film Sensor for In-Situ Monitoring of Structural Integrity of Laminated Composites, Key Engineering Materials Vol. 270-273, pp. 1929-1934

Loutas, T. H., Kostopoulos, V., Ramirez C. and Pharaoh, M. (2006) Damage Evolution in Center-Holed Glass/Polyester Composites Under Quasi-Static Loading Using Time/Frequency Analysis of Acoustic Emission Monitored Waveforms, Composites Science and Technology Vol. 66, pp. 1366-1375

Miller, R. K. and McIntire, P. (1987) Nondestructive Testing Handbook 2nd Edition, Volume 5 Acoustic Emission Testing, American Society for Nondestructive Testing

Misiti, M., Misiti, Y., Oppenheim, G. and Poggi, J. M. (2000) Wavelet Toolbox User's Guide, Version 2. Natik, MA, USA: The Math works, Inc.

Ni, Qing-Qing and Iwamoto, M. (2002) Wavelet Transform of Acoustic Emission Signals in Failure of Model Composites, Engineering Fracture Mechanics Vol. 69, pp. 717-728

Park, J., Kong, J., Kim, D. and Yoon, D. (2005) Nondestructive Damage Detection and Interfacial Evaluation of Single-Fiber/Epoxy Composites Using PZT, PVDF and P(VDF-TrFE) Copolymer Sensors, Composites Science and Technology, Vol. 65, pp. 241-256

Qi, Gang (2000) Wavelet-Based AE Characterization of Composite Materials, NDT&E International Vol. 33, pp. 133-144